

Magnetic structure of GdCu through the martensitic structural transformation: A neutron-diffraction study

J. A. Blanco

Departamento de Física, Universidad de Oviedo, 33007 Oviedo, Spain

J. I. Espeso, J. García Soldevilla, and J. C. Gómez Sal

Departamento de Ciencias de la Tierra y Física de la Materia Condensada, Facultad de Ciencias, Universidad de Cantabria, 39005 Santander, Spain

M. R. Ibarra and C. Marquina

Instituto de Ciencia de Materiales de Aragón and Departamento de Física de la Materia Condensada, Consejo Superior de Investigaciones Científicas, Universidad de Zaragoza, 50009 Zaragoza, Spain

H. E. Fischer

Institut Laue-Langevin, BP. 156, 38042 Grenoble Cédex 9, France

(Received 14 April 1998)

We report investigations on the magnetic structure through the martensitic structural transformation in the GdCu system obtained by means of neutron-diffraction experiments. At room temperature, the as-cast bulk samples adopt a CsCl-type crystallographic structure, but when the temperature is lowered a martensitic structural transformation CsCl→FeB takes place at around 250 K propagating down to 120 K. After a thermal cycle through the forward and the reverse transformation, at room temperature the percentage of both phases is found to be ~25% for the CsCl-type structure and ~75% for the FeB-type one. In contrast, in powdered samples the CsCl-type phase is stable at any temperature. A comparative neutron thermodiffraction study in both types of samples allows us to separate and investigate the magnetic behavior of these phases. The magnetic structure of the CsCl-type phase below $T_N^{\text{CsCl}} = 150$ K is most consistent with a simple antiferromagnetic one with a propagation vector $\mathbf{Q}^{\text{CsCl}} = (\frac{1}{2}, \frac{1}{2}, \mathbf{0})$, the magnetic moments lying along the *c* direction. However, for the FeB-type structure below $T_N^{\text{FeB}} = 45$ K, the situation is more complex: a helimagnetic structure with a propagation vector $\mathbf{Q}^{\text{FeB}} = (\mathbf{0}, \frac{1}{4}, \frac{1}{4})$ is proposed. Furthermore, it is concluded that while *RCu* cubic magnetic structures could be understood within a simple isotropic free-electron Ruderman-Kittel-Kasuya-Yosida model, an exchange anisotropy is needed in the orthorhombic GdNi_{1-x}Cu_x compounds to account for the evolution of the magnetic structures. Finally, an insight into the mechanism of the martensitic transformation is also discussed. [S0163-1829(99)08401-5]

I. INTRODUCTION

Since the 1960s, much of the interest in the intermetallic *RM* compounds (*R*=rare earth, *M*=no magnetic transition metal)¹⁻⁴ has been devoted to the interaction mechanism responsible for the magnetic coupling between the *R* ions: the isotropic bilinear exchange interaction which, in these intermetallic compounds, is mediated by conduction electrons. This so-called Ruderman-Kittel-Kasuya-Yosida (RKKY) interaction is known to be long range and oscillatory with distance. However, the differences among the magnetic behavior of equiatomic *RM* compounds cannot be attributed to internuclear separations only; the different type of magnetic ordering (ferro or antiferro) must be then driven mostly by the number of conduction electrons. In addition, the changes in this electron density could be also responsible for the existence of structural transformations in these compounds.

In particular, the equiatomic *RCu* series is characterized by the existence of a lattice instability. The light rare-earth-based compounds crystallize in the orthorhombic FeB-type structure, while the heavy ones do so in the cubic CsCl-type

structure. GdCu is the first in the series to adopt this cubic structure at room temperature, but is unstable showing a tendency to transform into a FeB-type one at low temperatures.⁵⁻⁸ This phase transition has been identified as a diffusionless thermoelastic martensitic transformation being characterized by a large thermal hysteresis at the pronounced volume and electrical resistivity anomalies.⁸⁻¹⁰ After a suitable heat treatment up to 800 K the CsCl-type structure is recovered. The same type of structural transformation was also found in YCu and Tb_xY_{1-x}Cu compounds¹¹⁻¹³ suggesting that the origin of these instabilities should not be related to *4f* magnetic effects. Recent results obtained from x-ray-absorption spectroscopy showed that the *s-d* hybridization plays a major role in driving this cubic-orthorhombic transformation.¹⁴ In contrast, for powdered GdCu samples x-ray and Mössbauer effect measurements down to 4.2 K showed that the CsCl-type structure is stable in the whole temperature range investigated, because the stress induced during the powdering process favors the CsCl-type structure.¹⁵

On the other hand, the equiatomic *RNi* compounds crys-

tallize within the CrB-type structure for $R=\text{La}$ to Gd , and within the FeB-type structure for $R=\text{Dy}$ to Tm . In this way, the substitution of Ni by Cu in the $\text{GdNi}_{1-x}\text{Cu}_x$ compounds leads to a structural transformation $\text{CrB} \rightarrow \text{FeB}$ for $x \geq 0.2$ and to a change from ferromagnetism to antiferromagnetism for $x \geq 0.35$.¹⁶ A thorough study of the magnetic structures of $\text{GdNi}_{1-x}\text{Cu}_x$ compounds ($x=0, 0.3, \text{ and } 0.6$) showed that for $x=0.6$ the magnetic structure is a simple helimagnetic with a propagation vector $\mathbf{Q}^{\text{FeB}} = (0, 0, \frac{1}{4})$, the magnetic moments lying in the \mathbf{ab} plane of the crystallographic structure.¹⁷ However, the mechanism that drives the magnetic order change in $\text{GdNi}_{1-x}\text{Cu}_x$ compounds is not yet completely understood.

The different temperature dependence of the bulk and powdered samples (with and without martensitic transformation, respectively), allows us to perform a comparative neutron-diffraction study of both samples, which is reported in this work.

Due to the high penetration depth of neutrons, this experiment provides a full picture of the crystal structure transformation in the whole sample, while previous x-ray studies^{7,8} reflect mainly surface transformations. This structural behavior strongly influences the macroscopic magnetic properties and neutron-scattering measurements are then essential to investigate the magnetic structures of the different phases in this system. This information will be necessary to establish a relation between the magnetism and the structural transformation in the GdCu system and in addition to have a deeper insight into the magnetic interactions of $\text{GdNi}_{1-x}\text{Cu}_x$ compounds.

This paper is organized as follows: Section II is devoted to the experimental details of sample preparation, x-ray and macroscopic characterizations. Neutron-diffraction results are given in Sec. III for both types of GdCu samples. Finally, Sec. IV is devoted to the analysis and discussion of the present results also considering those previously obtained.

II. SAMPLE PREPARATION AND EXPERIMENTAL DETAILS

A. Sample preparation and x-ray characterization

About 20 g of polycrystalline GdCu specimens were prepared by arc melting nominal 99.9% purity Gd and 99.99% nominal Cu in an inert atmosphere of purified Ar gas (the GdCu melting point is 830 °C). The samples were remelted several times, and subsequently wrapped in Ta foil and annealed under high vacuum at 800 °C for a week as was done by Sarusi *et al.*⁹ The samples were very malleable, being necessary to file them in order to obtain powdered samples.

Room-temperature x-ray powder-diffraction measurements revealed that the sample crystallizes in the CsCl-type phase. No other peaks corresponding to supplementary phases were detected. At room temperature, the cell parameter of the CsCl-type cubic structure was found to be 3.504(2) Å, which is very close to that previously published 3.502 Å.^{5,8,18} In addition, the stoichiometry and homogeneity of all the samples were analyzed by the x-ray dispersive analysis (XDA) technique and were found to be 52 ± 2 at. % Gd and 48 ± 2 at. % Cu in all the sample analyzed regions.

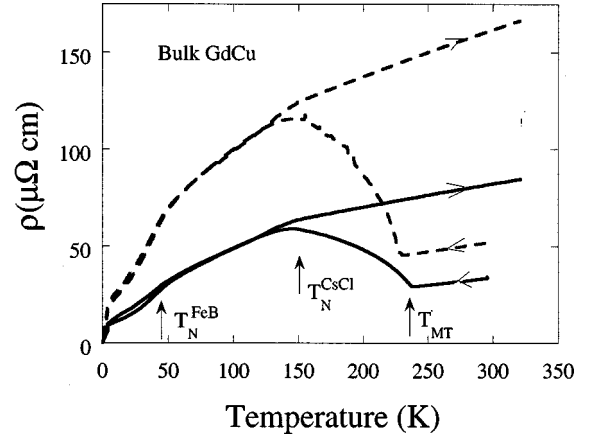


FIG. 1. Temperature dependence of the electrical resistivity for bulk GdCu. The arrows on the resistivity curves indicate the measuring direction. The vertical arrows denote the structural martensitic transformation, T_{MT} and the ordering temperatures of the CsCl-type, $T_{\text{N}}^{\text{CsCl}}$, and FeB-type, $T_{\text{N}}^{\text{FeB}}$, phases. The full line corresponds to the first resistivity measurement, while the dotted one corresponds to the same sample after annealing at 800 K during 10 h.

B. Macroscopic characterization: Resistivity and magnetization measurements

In order to make a macroscopic characterization of our bulk GdCu samples, we have performed resistivity by the ac four-probe method and magnetization measurements. In the former the contacts were made by pressure and the measurements were repeated several times. In Fig. 1 we show two different thermal cycles of the electrical resistivity ρ for GdCu. The first one corresponds to the as-cast bulk GdCu sample and the second one was obtained from the same specimen after annealing at around 800 K for 10 h. In both cases, the sample was firstly cooled from room temperature to 1.5 K and then heated up to room temperature, as shown by the arrows on the resistivity curves. The differences observed in the absolute values between both measurements are due to the propagation of microcracks in the samples, releasing the internal stress and leading to higher values of the resistivity. These measurements are in good agreement with those published previously.⁸ The negative $d\rho/dT$ behavior, observed in the temperature interval between 250 and 150 K, is ascribed to the progressive martensitic transformation into the FeB-type structure. The change of the slope $d\rho/dT$ at around 45 and 150 K is attributed to the magnetic ordering in the FeB-type and the CsCl-type phases, respectively. It is worth mentioning that in spite of the cracks propagation the main features of both curves are fully reproducible: $T_{\text{N}}^{\text{CsCl}}$, $T_{\text{N}}^{\text{FeB}}$, and the temperature range of the martensitic transformation. Furthermore, as the cracks propagation takes mainly place during the cooling process¹⁹ and both resistivity curves, which were measured while heating, collapse under normalization, it could be deduced that the annealing process does not modify the evolution of the nominal percentage of the crystalline phases.

In Fig. 2 we plot the ac magnetization, M' and M'' , versus temperature at 5 kHz measured in a bulk GdCu sample. Only clear evidence of the ordering temperature of the FeB-type phase, $T_{\text{N}}^{\text{FeB}}$, is detected, because at the Néel temperature of the CsCl-type structure, $T_{\text{N}}^{\text{CsCl}} = 150$ K, most of the

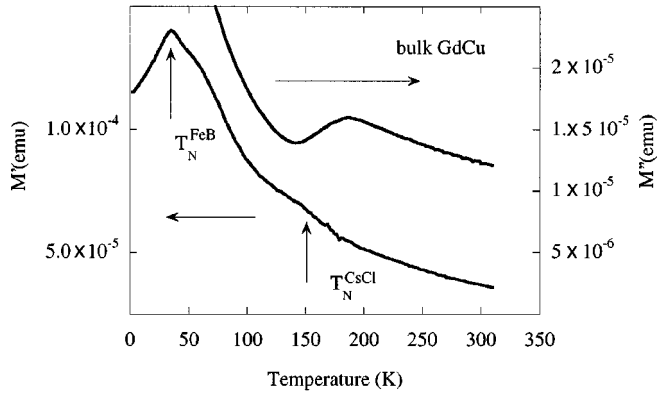


FIG. 2. Temperature dependence of ac magnetization M' and M'' at 5 kHz for bulk GdCu. The vertical arrows denote the ordering temperatures of the CsCl-type and FeB-type phases.

bulk sample has a FeB-type structure (see below). On the other hand, the hump observed in the imaginary component M'' between 250 and 150 K is also related to the martensitic transformation, confirming that this transition has a gradual character and it is accompanied by a considerable structural disorder of the lattice. The observed variations of the magnetization coincide to a high degree with those previously found.⁸

C. Neutron-diffraction experiments

The neutron absorption cross section of natural gadolinium is extremely high for thermal neutrons, but this absorption is significantly reduced for neutron wavelengths of $\lambda = 0.5 \text{ \AA}$. For this reason, neutron-diffraction experiments were performed on the *D4* diffractometer situated in the *H8* hot neutron beam working with a momentum transfer Q , $0.3 < Q/\text{\AA} < 24$ at the Institut Laue-Langevin in Grenoble. In normal operation the instrument which is on a Tanzboden, has two independent 2θ arms that cover, respectively, the low and high angle part of the scattering pattern. In the multidetectors, the cell spacing is such as to give 0.1° steps at a sample to detector distance about 1.5 m.

In order to investigate the magnetic structures of GdCu in both phases, the CsCl-type and the FeB-type, we have carried out experiments in powdered and bulk samples. Typical counting time was 5 h per spectrum. We have collected spectra on cooling at 300, 180, 140, 130, 120, 80, 40, and 5 K for powdered GdCu samples, which has only the CsCl-type structure, and in the same way we have recorded data at 300, 220, 180, 160, 120, 5, 20, 40, 80, 120, 140, 180, and 300 K in bulk GdCu samples in which both types of crystal structures coexist. The comparative analysis of these two experiments allows us to separate the contribution observed in the bulk GdCu spectra. For the analysis we have applied the Rietveld method to refine the nuclear and magnetic structures using the program FULLPROF.²⁰ The magnetic form factor of Gd^{3+} has been taken from Ref. 21, while Cu atoms are assumed to be nonmagnetic. We have used the scattering length $b_{\text{Gd}} = 1.2(1)10^{-12} \text{ cm}$ taken from previous works with comparable neutron wavelength.^{22,23} The refined parameters were: the scale factor, the cell parameters, the atomic positions of the Gd and Cu ions in the FeB orthorhombic

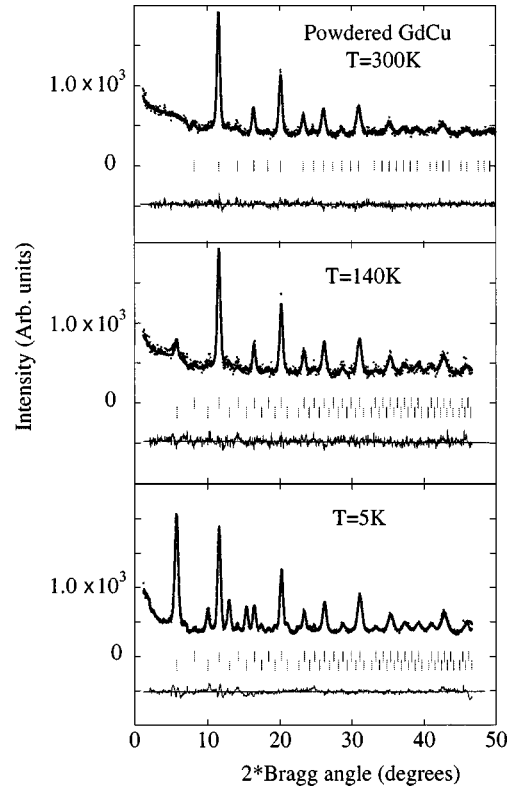


FIG. 3. Neutron-diffraction patterns of powdered GdCu sample at 300, 140, and 5 K, these patterns have been selected as the most characteristic among the set of measurements done. The solid line corresponds to the Rietveld refinements. The upper (lower) vertical marks are the nuclear (magnetic) peaks.

structure, the η parameter of the pseudo-Voigt profile shape function, and the components of the magnetic moments.

III. NEUTRON-DIFFRACTION RESULTS

A. Powdered GdCu samples: Cubic CsCl-type structure

Figure 3 shows the observed and calculated patterns of powdered GdCu samples obtained at 300, 140, and 5 K. The neutron-diffraction peaks observed at temperatures above $T_N^{\text{CsCl}} = 150 \text{ K}$ were easily indexed on a cubic CsCl-type unit cell. In all the spectra no peaks of the FeB-type structure were detected at any temperature confirming that the powdered samples have only a CsCl-type structure.

Below 150 K an additional set of reflections is observed, their intensity increasing when temperature is lowered. These new peaks have been indexed on the basis of a magnetic unit cell doubled along two cube edges. This is characteristic of an antiferromagnetic structure of the $(\pi, \pi, 0)$ -type,²⁴ i.e., propagation vector $\mathbf{Q}^{\text{CsCl}} = (\frac{1}{2}, \frac{1}{2}, 0)$. In order to account for the magnetic intensities the magnetic moments must be parallel to the c axis. However, it is important to note that this magnetic collinear antiferromagnetic structure and noncollinear (multiaxis) magnetic structures may give rise to the same neutron-diffraction patterns.²⁵ To remove this ambiguity further experiments on single crystals or Mössbauer spectroscopy are necessary. This situation was also found in heavy RCu compounds ($R = \text{Tb, Dy, Ho, Er, and Tm}$).²⁶ At low temperatures they order within the

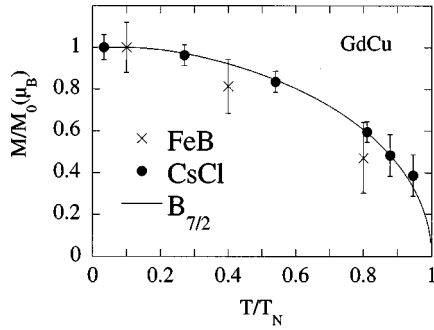


FIG. 4. Temperature dependence of the reduced ordered magnetic moment in GdCu samples. The solid line corresponds to the Brillouin function for $J=7/2$. The \bullet are the values of the magnetic moment of the powdered CsCl-type phase. For a comparison we have displayed the values obtained for the FeB-type GdCu phase (\times) in bulk samples.

$(\pi, \pi, 0)$ -type structure, while for most of them, near the Néel temperature, this ordering is replaced by a more complex one, resulting from the competition between crystalline electric field (CEF) and exchange interactions. In the present GdCu case the $(\pi, \pi, 0)$ equal moment structure remains stable throughout the whole temperature range.

On the other hand, the temperature dependence of the ordered Gd^{3+} magnetic moment obtained from our fittings of neutron-diffraction patterns in powdered samples is represented in Fig. 4 together with the theoretical variation obtained using a $B_{7/2}$ Brillouin function. The agreement between both variations is quite good indicating that the RKKY exchange interactions in this compound have an almost isotropic character. The results of the refinements are summarized in Table I. The inferior quality of the R_{mag} factor approaching the Néel temperature reflects the smaller values of the magnetic signal.

B. Bulk GdCu samples: Orthorhombic FeB-type structure

The neutron-diffraction patterns of bulk GdCu samples, collected from room temperature down to 5 K in the cooling process and heating process detailed above, are depicted in Figs. 5 and 6. At 300 K the pattern is quite well described considering only the CsCl-type structure but at 220 K the results are only consistent when the FeB-type one is also included in the refinements. The results at this temperature lead to a

TABLE I. Final parameters obtained from the neutron-diffraction profile refinements in a powdered GdCu sample (CsCl phase).

| T (K) | a (Å) | R_B (%) | M (μ_B) | R_{mag} (%) |
|---------|----------|-----------|-----------------|----------------------|
| 300 | 3.495(2) | 12.0 | | |
| 180 | 3.491(2) | 8.1 | | |
| 140 | 3.488(3) | 7.9 | 2.8 ± 0.1 | 34.5 |
| 130 | 3.485(1) | 7.0 | 3.5 ± 0.1 | 14.5 |
| 120 | 3.484(1) | 5.1 | 4.31 ± 0.05 | 10.7 |
| 80 | 3.483(1) | 6.6 | 6.05 ± 0.05 | 6.7 |
| 40 | 3.480(1) | 7.5 | 6.97 ± 0.05 | 8.5 |
| 5 | 3.481(1) | 7.0 | 7.24 ± 0.06 | 9.1 |

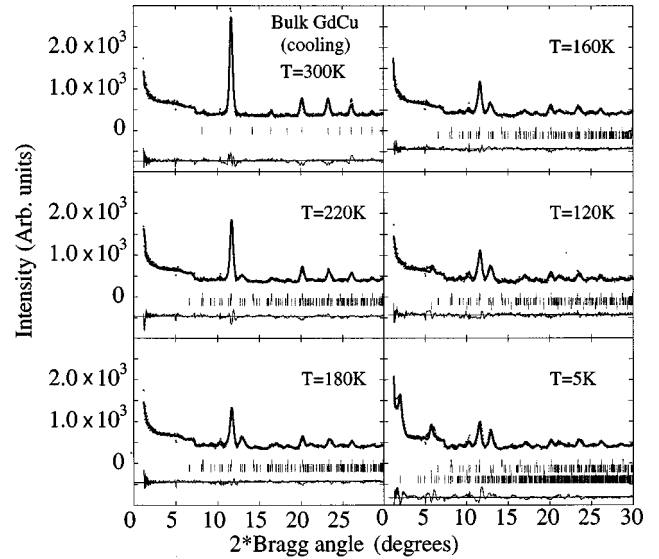


FIG. 5. Neutron-diffraction patterns of the bulk GdCu sample at 300, 220, 180, 160, 120, and 5 K in the cooling process. The solid line corresponds to the Rietveld refinements. The upper and lower marks at 220, 180, and 160 K are associated with the CsCl and the FeB-type structures, respectively. Below 150 K the third vertical marks correspond to the magnetic structure of the CsCl-type phase and finally below 40 K the fourth vertical marks are due to the magnetic phase of the FeB-type one.

percentage of each phase of 62 and 38%, respectively. When the temperature is lowered the percentage of the FeB-type structure increases progressively and reaches approximately the value of 75% below 120 K. The corresponding phase percentages extracted from the fittings of neutron patterns along the thermal cycle are presented in Fig. 7. The final crystallographic parameters appear in Table II. The relatively poor refinements in the FeB and CsCl phases in the bulk sample together with the slight differences observed in the lattice parameters of the CsCl-type phase between powdered and bulk samples result from the difficulty in describing both

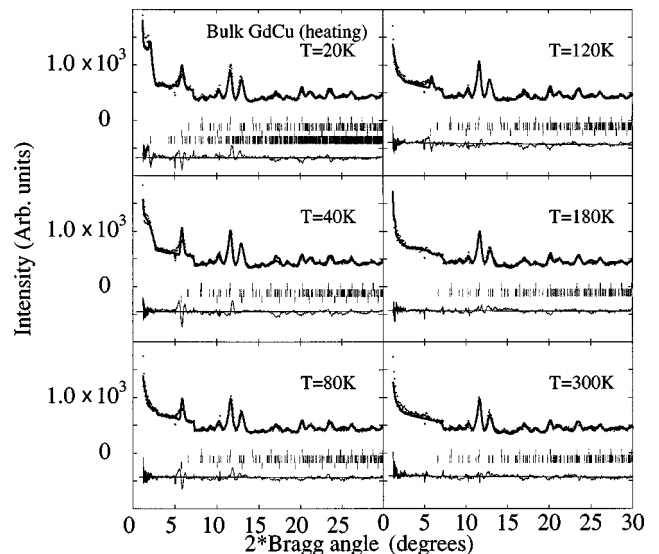


FIG. 6. Neutron-diffraction patterns of bulk GdCu sample at 20, 40, 80, 120, 180, and 300 K in the heating process. The marks follow the same criteria as in Fig. 5.

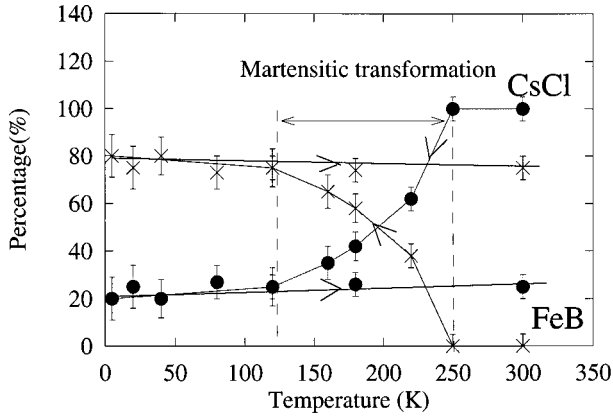


FIG. 7. Temperature dependence of the percentage of the CsCl-type and the FeB-types structures in bulk GdCu samples. Lines are visual guides.

phases accurately due to the problems of the peak shape and the strong effect of coarse grains, inherent to the nature of our sample. At this point it is worth mentioning that the quality of the refinements are clearly improved after the thermal cycle described in Sec. II C (see Table II and Figs. 5 and 6).

The temperature dependence of the GdCu unit cell of both types of structures is shown in Fig. 8. At room temperature, the FeB-type structure has a volume larger than that of the CsCl-type one, but quite similar at low temperatures. The absence of any crossover of the cell volumes (see Fig. 8) seems to indicate that the volume contraction is not the driving parameter for the martensitic transformation. However, in order to ascertain this circumstance more precise data about the coordination environments, details of bond distances, etc. are needed in the vicinity of $T_{MT}=250$ K.

As can be seen in Figs. 5 and 6 the analysis of the patterns below 150 K have been carried out taking into consideration the magnetic structure of the CsCl phase ($\pi, \pi, 0$) with the fixed characteristics obtained for the powdered sample (Table I), and below 50 K the magnetic structure of the FeB phase must be also considered. Concerning the magnetic

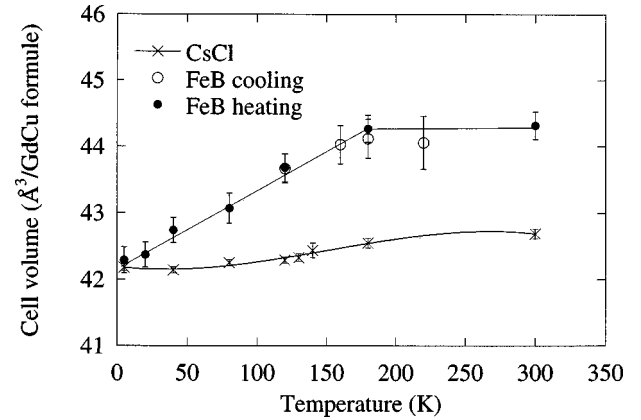


FIG. 8. Temperature dependence of the GdCu unit cell for the CsCl-type and the FeB-type phases. Lines are visual guides.

structure of the FeB-type phase, it is worth noticing that the magnetic peak observed around $2\theta=2^\circ$ [see Fig. 5 ($T=5$ K) and Fig. 6 ($T=20$ K)] can be indexed with a propagation vector $\mathbf{Q}^{FeB}=(0, \frac{1}{4}, \frac{1}{4})$ in the orthorhombic cell. Due to the poor resolution at $\lambda=0.5$ Å in $D4$, which prevents a straightforward separation of the magnetic peaks (see Figs. 5 and 6), it is quite difficult to ascertain the actual magnetic structure model of the FeB-type phase. Many different attempts with magnetic arrangements (sine-wave-modulated, antiphase, etc.) were unsuccessfully undertaken considering the $(0, \frac{1}{4}, \frac{1}{4})$ periodicity. However, regarding the helimagnetic structure of the $GdNi_{0.4}Cu_{0.6}$ compound, which is close to GdCu in composition and with the same FeB structure, we have tried a helimagnetic structure with a propagation vector $(0, \frac{1}{4}, \frac{1}{4})$ for the GdCu (FeB) phase. This structure is that which offers the closest agreement with the experimental pattern out of all the considered possibilities. The magnetic intensities are consistent with a magnetic moment of $7.0\mu_B$ at 5 K for the Gd^{3+} in the FeB-type GdCu phase, with the magnetic moments lying in the plane perpendicular to the $[011]$ direction. The temperature dependence of this magnetic moment is also shown in Fig. 4, and in spite of the larger error bar, it agrees also with the $B_{7/2}$ Brillouin law.

TABLE II. Final crystallographic parameters obtained from the neutron-diffraction profile refinements in bulk GdCu sample. The atomic positions of the FeB-type GdCu structure were found to be: Gd, $x=0.185(3)$, $z=0.150(3)$; Cu, $x=0.027(4)$, $z=0.625(4)$.

| T (K) | GdCu (CsCl-type) | | | GdCu (FeB-type) | | | | |
|---------|------------------|--------------|-----------|-----------------|-----------|-----------|--------------|-----------|
| | a (Å) | Percent. (%) | R_B (%) | a (Å) | b (Å) | c (Å) | Percent. (%) | R_B (%) |
| 300 | 3.492(2) | 100(5) | 18.0 | | | | | |
| 220 | 3.496(2) | 62(5) | 18.4 | 7.13(3) | 4.527(16) | 5.46(2) | 38(5) | 22.4 |
| 180 | 3.496(3) | 42(6) | 21.2 | 7.14(2) | 4.519(9) | 5.47(1) | 58(6) | 19.5 |
| 160 | 3.493(3) | 35(7) | 21.8 | 7.15(2) | 4.511(9) | 5.46(1) | 65(7) | 22.8 |
| 120 | 3.481(3) | 25(8) | 19.3 | 7.12(1) | 4.502(8) | 5.45(1) | 75(8) | 19.1 |
| 5 | 3.480(2) | 20(9) | 14.2 | 7.05(1) | 4.406(7) | 5.446(9) | 80(9) | 15.7 |
| 20 | 3.489(6) | 25(9) | 21.0 | 7.03(1) | 4.431(7) | 5.441(8) | 75(9) | 17.0 |
| 40 | 3.481(3) | 20(8) | 23.6 | 7.02(1) | 4.476(7) | 5.441(8) | 80(8) | 20.0 |
| 80 | 3.471(3) | 27(7) | 25.0 | 7.09(1) | 4.475(9) | 5.430(10) | 73(7) | 24.3 |
| 120 | 3.481(2) | 25(5) | 22.1 | 7.09(1) | 4.508(8) | 5.466(9) | 75(5) | 22.0 |
| 180 | 3.496(3) | 26(5) | 16.1 | 7.15(1) | 4.527(8) | 5.471(8) | 74(5) | 17.8 |
| 300 | 3.495(3) | 25(5) | 11.8 | 7.13(1) | 4.522(8) | 5.498(8) | 75(5) | 14.9 |

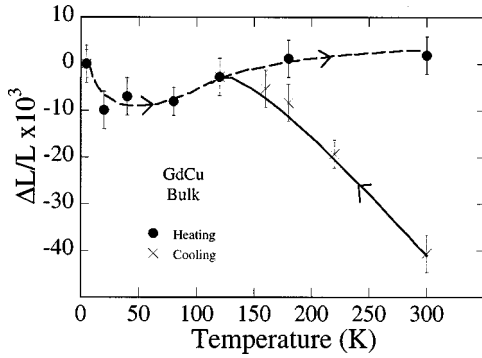


FIG. 9. Average thermal expansion $\Delta L/L$ of the bulk GdCu extracted from the data of crystallographic refinements (Table II). Lines are visual guides.

IV. ANALYSIS AND DISCUSSION

The combined structural and magnetic characterization carried out gives a clearer description of the phase stability of this system, especially in the bulk sample where both structural (CsCl and FeB) and magnetic $[(\pi, \pi, 0)$ and helimagnetic $(0, \frac{1}{4}, \frac{1}{4})]$ phases coexist at low temperatures (see Figs. 4, 7, and 8). This analysis has been possible due to a careful characterization of the magnetic structure of the CsCl phase (powdered sample) which permits microscopic information about the magnetism of the FeB phase of GdCu to be obtained. The soundness of this microscopic analysis can be remarked through the comparison with previous macroscopic results. In this way the detailed neutron data (Table II and Figs. 7 and 8) allow us to estimate the variation of the average thermal expansion (Fig. 9) which reproduces with excellent agreement the macroscopical thermal-expansion measurements reported in Ref. 10, showing that the changes in volume are associated with the martensitic structural transformation CsCl \rightarrow FeB in bulk samples. Furthermore, several relevant points regarding the martensitic transformation itself and the evolution of the magnetic structure in GdNi $_{1-x}$ Cu $_x$ compounds can be underlined from this study. The first comment of the discussion concerns the structural transition. It has been well established that such a transition takes place by means of a martensitic transformation, which is not related to the onset of the magnetic order.^{8,10,12,13} Our neutron-diffraction experiments, especially the temperature dependence of the lattice parameters in the powdered samples, without any anomaly (see Table I) suggests that the transition CsCl \rightarrow FeB is completely suppressed in the whole powdered sample, and not only on the surface. In fact, previous x-ray analysis⁸ only probes the sample surface. On the other hand, in bulk samples, when the martensitic transformation takes place, we found a coexistence of both phases. At 5 K the CsCl phase is still present around $\sim 20\%$, maintaining this percentage throughout the heating back up to room-temperature process.

The second important point is related to the magnetic structure of the CsCl-type GdCu phase. As well as for the other RCu compounds, GdCu orders with a $(\pi, \pi, 0)$ -type arrangement, although the actual direction of the magnetic moments is not definitively well established for GdCu. However, this case is quite interesting in order to clarify the role of the CEF and the exchange interactions for determining the direction of the magnetic moments in the RCu compounds. The fact that almost all of these compounds have, at least at low temperatures, $\mathbf{Q}^{\text{CsCl}} = (\frac{1}{2}, \frac{1}{2}, 0)$ as propagation vector, indicates continuity and a link through the full series. This feature could be understood within the framework of a simple RKKY model considering the conduction electrons as free electrons.²⁷ Under these assumptions the Fourier transform of the bilinear exchange interaction, $J(q)$, could be easily calculated for different spin arrangements as a function of the Fermi wave vector k_F (see Fig. 2 of Ref. 27). For the case of GdCu, k_F could be estimated to be $0.69 (2\pi/a)$ and for this value the antiferromagnetic structure of $(\pi, \pi, 0)$ -type is the most stable one. This indicates that the $J(q)$ variation has a marked maximum around \mathbf{Q}^{CsCl} through all the RCu series, and the existence of these structures for the CsCl phases is mainly due to the isotropic exchange interactions in lieu of CEF effects.

The third important aspect to be mentioned concerns the FeB-type GdCu phase and the related GdNi $_{1-x}$ Cu $_x$ compounds. The main magnetic properties of these orthorhombic GdNi $_{1-x}$ Cu $_x$ are presented in Table III. When the Cu concentration increases a transition from ferromagnetism ($x = 0.3$) to antiferromagnetism ($x = 0.6$ and 1.0) is developed. In addition, the magnetic moment M is along the \mathbf{b} axis in the ferromagnetic compounds and changes towards a direction lying in a plane perpendicular to $[011]$ for $x = 1$. To explain this modification some kind of anisotropic interactions must be considered. As Gd³⁺ has $L = 0$, the CEF is expected to be almost negligible in first order. The anisotropy could originate from the low symmetry of the crystal-line structure and its effect on the conduction band, which is responsible for the propagation of the magnetic interactions. In particular, the variation of the ordering ($T_{C,N}$) or paramagnetic Curie (θ_p) temperatures¹⁷ confirms the importance of this anisotropy. It is clear that as the interaction is not isotropic, the simple model of Ref. 27 is no longer valid. Then the present results strongly support a profound revision of this model in order to take into account the actual shape of the Fermi surface to explain how the magnetic interactions are propagated from one site to another through the conduction band when the Ni ions are substituted by the Cu ones.

In conclusion, this study points out the differences in the magnetic properties of the cubic and orthorhombic GdCu phases. A joint analysis of neutron-diffraction experiments on powdered and bulk samples has allowed us to investigate

TABLE III. Magnetic properties of FeB-type GdNi $_{1-x}$ Cu $_x$ compounds.

| x | Type of ordering | $T_{C,N}$ (K) | θ_p (K) | Propag. vector | Direction of magnetic moments |
|-----|------------------|---------------|----------------|----------------|-------------------------------|
| 0.3 | F | 68 | 75 | (0, 0, 0) | $M \parallel [010]$ |
| 0.6 | AF | 63 | 69 | (0, 0, 1/4) | $M \perp [001]$ |
| 1.0 | AF | 48 | -40 | (0, 1/4, 1/4) | $M \perp [011]$ |

the magnetic structure of both systems. While a simple RKKY model based on a spherical Fermi surface can be used to understand the stability of the $(\pi, \pi, 0)$ -type magnetic phase in the cubic GdCu, we found that this model cannot adequately describe the change of magnetic behavior in the orthorhombic $\text{GdNi}_{1-x}\text{Cu}_x$ compounds. This feature suggests that the topology of the Fermi surface in this orthorhombic system seems to be quite relevant in order to explain the anisotropy observed in the magnetic interactions. This confirms the importance of electronic effects on the stability of structural and magnetic orderings on these RM

compounds. Further theoretical studies on this problem could consider this system as a model one.

ACKNOWLEDGMENTS

We are very grateful to Professor A. del Moral and C. Ritter for fruitful discussions. We wish to acknowledge the support of the Spanish Comision Interministerial de Ciencia y Tecnología (Research Project No. MAT96-1023-C03-02&03).

-
- ¹H. R. Kirchmayr and C. A. Poldy, in *Handbook on the Physics and Chemistry of Rare Earths*, edited by K. A. Gschneidner, Jr. and L. Eyring (North-Holland, Amsterdam, 1979), Vol. 2, p. 55.
- ²K. H. J. Buschow, in *Ferromagnetic Materials*, edited by E. P. Wohlfarth (North-Holland, Amsterdam, 1980), Vol. 1, p. 297.
- ³J. J. M. Franse and R. J. Radwansky, in *Handbook of Magnetic Materials*, edited by K. H. J. Buschow (North-Holland, Amsterdam, 1993), Vol. 7, p. 307.
- ⁴J. M. Fournier and E. Gratz, in *Handbook on the Physics and Chemistry of Rare Earths*, edited by K. A. Gschneidner, Jr. and L. Eyring (North-Holland, Amsterdam, 1993), Vol. 17, p. 409.
- ⁵A. Iandelli and A. Palenzona, in *Handbook on the Physics and Chemistry of Rare Earths* (Ref. 1), p. 1.
- ⁶C. C. Chao, H. L. Luo, and P. Duwez, *J. Appl. Phys.* **35**, 257 (1979).
- ⁷H. W. de Wijn, K. H. J. Buschow, and A. M. van Dierper, *Phys. Status Solidi* **30**, 759 (1968).
- ⁸J. C. van Dongen, T. T. Palstra, A. F. J. Morgownik, J. A. Mydosh, B. M. Geerken, and K. H. J. Buschow, *Phys. Rev. B* **27**, 1887 (1983).
- ⁹G. Sarusi, Y. Gefen, and J. Baron, *Philos. Mag. B* **53**, 583 (1986).
- ¹⁰R. M. Ibarra, T. S. Chien, and A. S. Pavlovic, *J. Less-Common Met.* **153**, 233 (1989).
- ¹¹M. R. Ibarra, P. A. Algarabel, and A. S. Pavlovic, *J. Appl. Phys.* **67**, 4814 (1990).
- ¹²C. Ritter, R. M. Ibarra, and R. M. Ibberson, *J. Phys.: Condens. Matter* **4**, L39 (1992).
- ¹³R. M. Ibarra, C. Marquina, C. Ritter, and A. S. Pavlovic, *J. Magn. Magn. Mater.* **104&107**, 1373 (1992).
- ¹⁴J. Chaboy and M. R. Ibarra, *Phys. Rev. B* **52**, 3206 (1995).
- ¹⁵J. W. Ross and J. Sigalas, *J. Phys. F* **5**, 1973 (1975).
- ¹⁶D. Gignoux and J. C. Gómez Sal, *J. Magn. Magn. Mater.* **1**, 203 (1976).
- ¹⁷J. A. Blanco, J. C. Gómez Sal, J. Rodríguez-Fernández, D. Gignoux, D. Schmitt, and J. Rodríguez-Carvajal, *J. Phys.: Condens. Matter* **4**, 8233 (1992).
- ¹⁸E. Burzo, I. Ursu, and J. Pierre, *Phys. Status Solidi B* **51**, 463 (1972).
- ¹⁹J. A. Blanco, D. Gignoux, J. C. Gómez Sal, J. Rodríguez-Fernández, J. Voiron, and J. M. Barandiaran, *J. Phys.: Condens. Matter* **2**, 677 (1990).
- ²⁰J. Rodríguez-Carvajal, *Physica B* **192**, 55 (1993).
- ²¹C. Stassis, H. W. Deckman, B. N. Harmon, J. P. Desclaux, and A. J. Freeman, *Phys. Rev. B* **15**, 369 (1977).
- ²²J. S. Abell, J. X. Boucherle, R. Osborn, B. D. Rainford, and J. Schweizer, *J. Magn. Magn. Mater.* **31-34**, 247 (1983).
- ²³J. M. Barandiaran, D. Gignoux, D. Schmitt, J. C. Gómez Sal, J. Rodríguez-Fernández, P. Chieux, and J. Schweizer, *J. Magn. Magn. Mater.* **73**, 233 (1988).
- ²⁴H. A. Gersch and W. C. Koehler, *Phys. Chem. Solids* **5**, 180 (1958).
- ²⁵M. Wintemberger and R. Chamard-Bois, *Acta Crystallogr., Sect. A: Cryst. Phys., Diffr., Theor. Gen. Crystallogr.* **A28**, 341 (1972).
- ²⁶P. Morin and D. Schmitt, *J. Magn. Magn. Mater.* **21**, 243 (1980).
- ²⁷J. Sakurai, Y. Kubo, T. Kondo, J. Pierre, and E. F. Bertaut, *J. Phys. Chem. Solids* **34**, 1305 (1973).